

TaS₂ nanoplatelets produced by laser ablation

Ka Yee Chick, Manashi Nath, and B.A. Parkinson^{a)}

The Department of Chemistry, Colorado State University, Fort Collins, Colorado 80523

(Received 2 November 2005; accepted 31 January 2006)

Tantalum disulfide (TaS₂) nanoplatelets were produced by laser ablation of a TaS₂ target under an argon atmosphere. The nanoplatelet dimensions and morphology were characterized by transmission electron microscopy and x-ray diffraction. The effect of the ablation laser power density on the size distribution of the nanoplatelets was studied. The TaS₂ nanoplatelets were prone to oxidation upon exposure to air but could be stabilized by using 3-mercaptopropionic acid as the capping agent.

I. INTRODUCTION

Layered transition metal dichalcogenides (TMD) have a structure similar to graphite, however, each graphene sheet is replaced by an MX₂ layer containing the transition metals (such as Ta, W, and Mo) in a trigonal prismatic or octahedral coordination sandwiched by layers of chalcogen atoms.¹ Nanosized TMD materials tend to fold into closed structures to reduce the energy of the dangling bonds, thus a range of closed-cage structures such as multishell onion-like clusters, generically called inorganic fullerenes, have been prepared.² Nanotubes,^{3,4} nanowires, and nanoribbons can also be obtained.⁵ TMD nanomaterials have a wide range of chemical and physical properties that make them attractive for many applications.^{6–9} TMD materials can be semiconducting, metallic, or even superconducting.¹

There are a variety of synthetic methods for producing TMD nanomaterials. Nanotubes have been synthesized by gas-phase methods,^{2,3} template methods,¹⁰ and sonochemical methods.¹¹ Inorganic fullerene materials can be prepared by a gas-phase method,¹² electron irradiation,¹³ or by laser ablation.^{12,14–17} Nanoplatelets of MoS₂ and InSe can be prepared via solution chemistry.^{18,19} Laser ablation, commonly applied in mass spectrometry²⁰ and for thin film deposition,²¹ is a nonequilibrium growth process useful for synthesizing nanomaterials and was used in the discovery of C₆₀.²² Laser ablation for nanoparticle production can take place under an inert gas environment^{14,15} or in a liquid medium.¹⁶ In the case of laser ablation under an inert gas, the laser beam removes material from the surface of the target by vaporization. Subsequently, during the adiabatic cooling process of the vaporized target material, nanoparticles can be formed.

In this article, we report the production of TaS₂ nanoplatelets via laser ablation of a TaS₂ target in an argon gas environment and we investigate the size distribution of the TaS₂ nanoplatelets as a function of the laser power. We also report the stabilization of solution suspensions of TaS₂ nanoplatelets by 3-mercaptopropionic acid (3-MPA).

II. EXPERIMENTAL METHOD

TaS₂ powder (99.9% Ta) was purchased from Strem Chemicals, Inc. (Newburyport, MA) and was used without further purification. 3-MPA was purchased from Aldrich (Milwaukee, WI) and was also used without further purification. Copper transmission electron microscopy (TEM) grids, with lacey Formvar/carbon polymer as the support film, were purchased from Ted Pella, Inc. (Redding, CA). TEM was carried out on a 2000 TEM (JEOL, Tokyo, Japan), operating at an accelerating voltage of 100 to 200 kV. Powder x-ray diffraction (XRD) of the samples was carried out on a D-8 Discover x-ray diffractometer (Cu x-ray source, line focus; Bruker, Billerica, MA) with a Göbel mirror on the primary beam side and a scintillation detector on the diffracted beam side. The angle of incidence was 0.5° and the measurements were performed with soller slits. Topas P, version 1.0.1, was used as the profile fitting software for the size analysis of the nanoplatelets.

A pulsed Nd:YAG laser (DCR11; Spectra-Physics, Mountain View, CA), with a fundamental wavelength at 1064 nm, was used as the laser source. It was operated in the Q-switch mode at 10 Hz with a 9-ns pulse width. The laser average output power was set between 0.1 and 2.6 W, resulting in a peak power between 1.1 and 29 megawatts (MW). A 40-cm focal length lens was used to converge the laser beam to the spot close to 3 mm in diameter. Therefore, the laser pulse energy density was calculated to be between 16 and 410 MW cm⁻².

^{a)}Address all correspondence to this author.

e-mail: Bruce.Parkinson@colostate.edu

DOI: 10.1557/JMR.2006.0148

TaS₂ powder (5–6 g) was pressed into a 33-mm diameter pellet. The as-prepared pellet was clipped to a sample holder located in the reaction chamber equipped with an optical window. The reaction chamber was first pumped down to a pressure below 50 mTorr before filling it with 200 Torr of argon. This argon pressure was found to be optimum for the preparation of the nanoplatelets. To increase the efficiency of ablation, the sample holder was attached to a motor to rotate the TaS₂ pellet during the experiment, thus allowing more areas on the pellet to be ablated. A TEM grid was placed in the reaction chamber to collect samples generated from the laser ablation. The laser ablation was started after 10 minutes of purging or when the Ar pressure inside the reaction chamber stabilized. The duration of a typical laser ablation run was 20 minutes.

III. RESULTS AND DISCUSSION

Laser ablation of the TaS₂ target produced black soot-like material. Figures 1(a)–1(c) show the TEM images of the soot collected in the reaction chamber at various laser

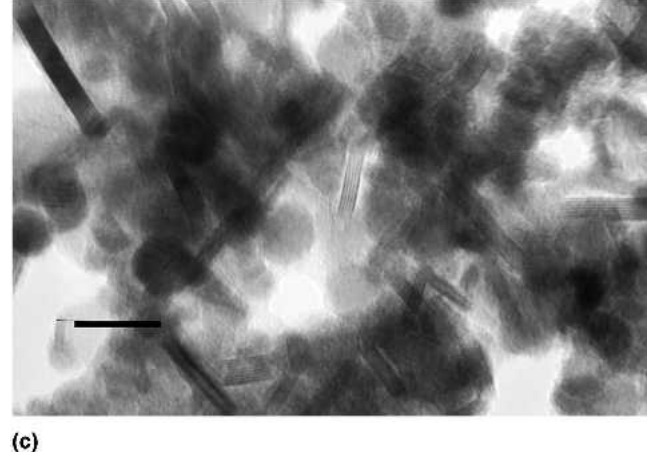
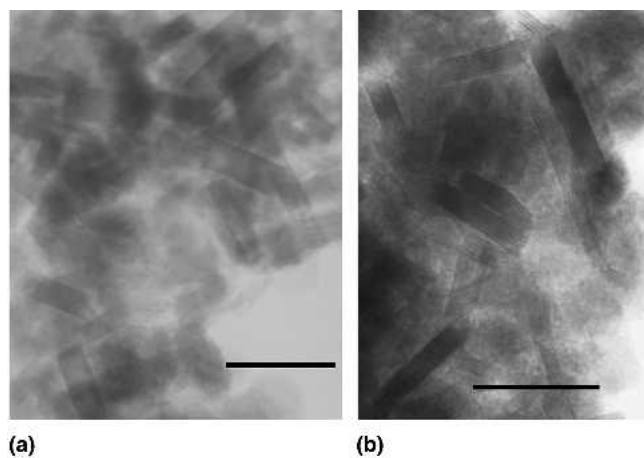


FIG. 1. TEM images of TaS₂ nanoplatelets produced at different laser power densities: (a) 409 MW cm⁻², (b) 79 MW cm⁻², and (c) 28 MW cm⁻². The scale bar in each image is to 20 nm.

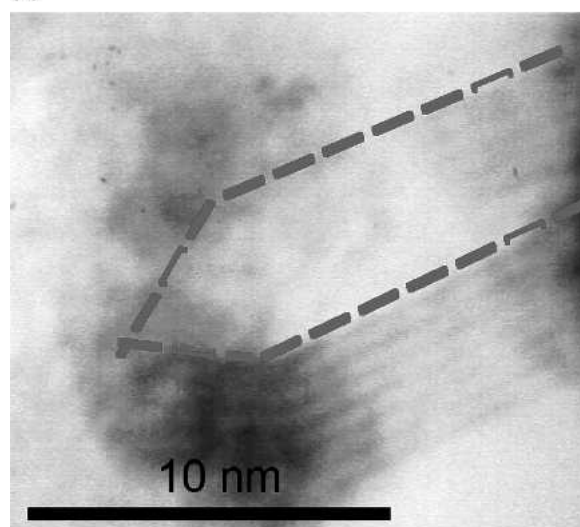
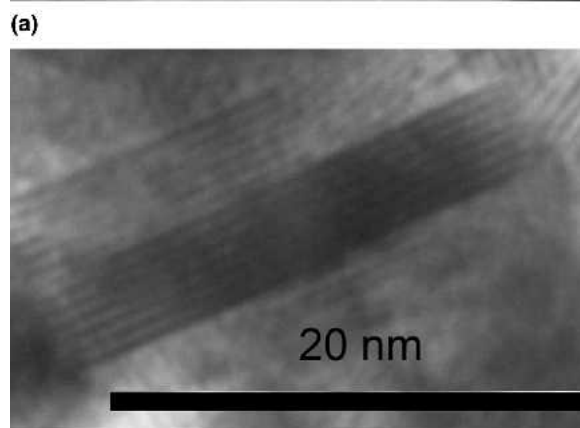
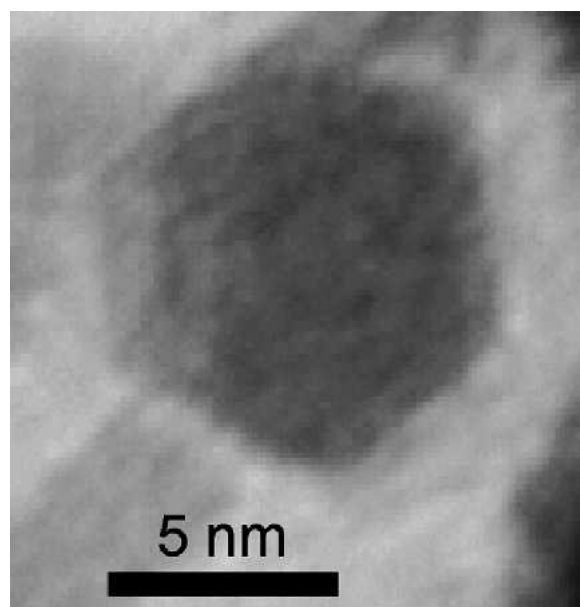


FIG. 2. High-magnification TEM images of different hexagonal TaS₂ nanoplatelets in various orientations: (a) top view, (b) side view, and (c) oblique angle (all nanoplatelets shown here were produced with a laser power density of 409 MW cm⁻²).

power densities. The TEM images revealed that hexagonal nanoplatelets were the dominant product, however, some nanospheres were also seen. Figures 2(a)–2(c) show the TEM images of TaS₂ nanoplatelets oriented at different angles that clearly are projections of the hexagonal form of the platelets. Tilting experiments in the TEM also verified the hexagonal structure. The interlayer distances in the nanoplatelets, obtained from the TEM lattice fringes, were between 6.50 and 5.50 Å, whereas the bulk TaS₂ materials has an interlayer distance of 5.94 Å.¹

The edge lengths of the nanoplatelets were also measured from the TEM images. Figures 3(a)–3(d) show the histograms of size distributions of nanoplatelets produced at various laser power densities. It can be seen that the laser pulse energy density has an effect on the size distribution of the nanoplatelets. Comparing the histograms of Fig. 3(a) to 3(d) shows that smaller nanoplatelets with a narrower size distribution were produced at a higher laser power density. One could speculate that the higher laser power densities produce a higher pressure plasma, resulting in a faster adiabatic expansion of the vaporized plume, and thus a higher cooling rate, resulting in a shorter growth time for the nucleated nanoparticles and thus a narrower size distribution.

One can also speculate about the mechanism of growth of the TMD nanoparticles. The high-power densities in the initial stage of ablation results in complete vaporization of a portion of the target material. The subsequent adiabatic expansion cools the plume, resulting in an initial nucleation and growth of the least volatile component

of the plume, in this case, Ta metal. The Ta metal nanoparticles are still engulfed in an environment of hot chalcogenide vapor, resulting in a reaction to form TaS₂ nanoparticles. If the Ta nanoparticles in the plume are hexagonal, a reasonable morphology for a metal crystal, a hexagonal nanoplatelet, is then templated. Octahedral nanoparticles of MoS₂, previously prepared by laser ablation of an MoS₂ target,²³ could be formed from a reaction of an octahedral nanocrystal of Mo templating the MoS₂ layers from subsequent reaction with sulfur vapor.

The powder XRD pattern of material generated by the laser ablation power density of 158 MW cm⁻², and containing a large fraction of nanoplatelets, revealed diffraction peaks associated with TaS₂ [Fig. 4(a)].²⁴ Analyzing the peak broadening observed for a particular TaS₂ powder XRD peak using the Scherrer method (profile-fitting program, Topas P, version 1.0.1) gives an average particle size of 18.8 nm. The same sample of nanoplatelets analyzed with TEM images showed sizes between 6 and 20 nm [Fig. 3(b)].

The TaS₂ nanoplatelets generated by laser ablation were not very stable under ambient conditions. The powder XRD pattern in Fig. 4(a) was obtained immediately after the synthesis. Exposure of the same sample to air for 1 day produced a different powder XRD pattern, showing that the TaS₂ converted to TaO₂ and Ta₂O₅ [Fig. 4(b)]. The powder XRD results were reproducible for all experiments, with variations in the tantalum sulfide and tantalum oxide ratio. TEM images, after samples were exposed to air, lose their clarity as the sample

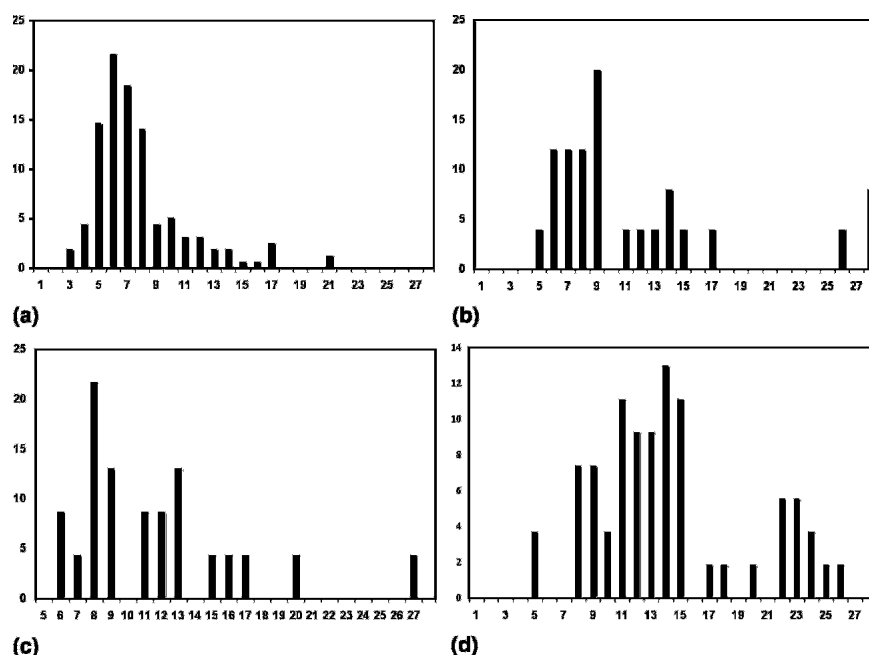


FIG. 3. Histograms of the size distribution of nanoplatelets produced at different laser power densities: (a) 409 MW cm⁻², (b) 158 MW cm⁻², (c) 79 MW cm⁻², and (d) 28 MW cm⁻² [x axis, platelet length (nm); y axis: frequency (%)].

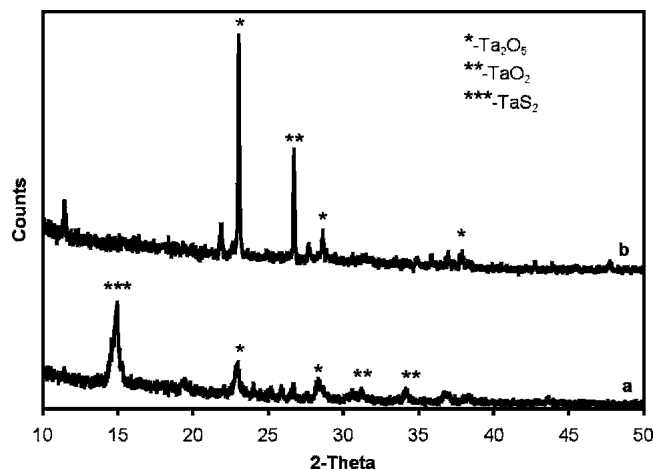


FIG. 4. XRD patterns of the nanomaterials (a) collected immediately after opening the chamber and (b) after the product was kept in air for 1 day. Unlabeled peaks could not be identified. (The nanoplatelets were produced with a laser power density of 409 MW cm⁻².)

degrades with time because of conversion to the oxide, and no longer showed the lattices fringes associated with the nanoplatelet's 5.50 to 6.50 Å interlayer distances.

Stabilizing the nanostructures with a capping agent could possibly reduce the oxidation rate of the TaS₂ nanoplatelets. Many other nanomaterials have been stabilized by capping agents.^{25,26} The oxidation of the nanoplatelets most likely starts with the dangling bonds at the edge of the nanoplatelets because the hexagonal faces are rather inert van der Waals surfaces. Therefore, we attempted to react the dangling bonds associated with the tantalum edge states with a thiol-containing ligand.

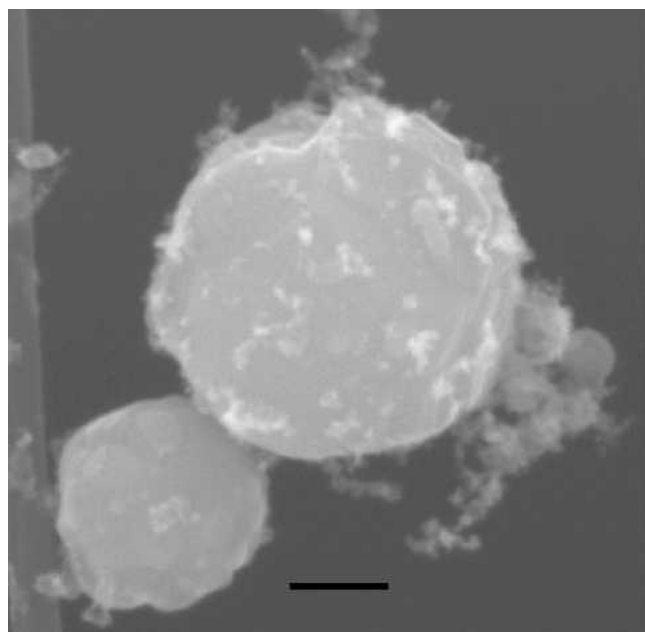


FIG. 5. SEM image of nanospheres produced by laser ablation at 330 MW/cm⁻² of laser power density. The scale bar is 100 nm.

3-MPA was chosen as the capping agent because we are also interested in producing a charge on the platelets to disperse the nanoplatelets and to stabilize the solution as a colloid. TaS₂ nanoplatelets generated from the laser ablation were collected from the reaction chamber and soaked in a 1.4 M aqueous solution of the sodium salt of 3-MPA. TEM images of the nanoplatelets, which were kept for 8 days in the aqueous 3-MPA solution exposed to air, showed fringes of the usual spacing, indicating that the TaS₂ nanoplatelets were successfully stabilized for at least 1 week by the 3-MPA solution.

As discussed above, the laser power density affected the particle size. Lower laser power densities also produced a higher percentage of spherical nanoparticles among the nanoplatelets. The spherical nanoparticles showed a wide range of diameters from 10 to 500 nm. Energy dispersive x-ray spectroscopy analysis of the nanospheres revealed that they were composed of tantalum and sulfur, but were tantalum rich. Lattice fringes were observed in TEM images in different domains on the surface of the sphere, however, the fringe interlayer distances were not uniform, even on the same nanosphere. Those nanospheres could be the produced when the droplets of melted Ta produced by the laser only partially reacted with sulfur during cooling. The lower laser power density results in some tantalum liquid droplets rather than complete vaporization as discussed in the mechanism above. The tantalum droplets are then only partially reacted with sulfur, resulting in Ta-rich spherules. An SEM image, shown in Fig. 5, shows that the surface of a nanosphere is not smooth. This suggests that some nanoclusters can aggregate on the surface of the nanospheres.

IV. CONCLUSIONS

We have demonstrated the synthesis of nanoplatelets of TaS₂ via laser ablation in an Ar atmosphere. The size distribution of nanoplatelets was dependent on the laser power density. Spherical tantalum-rich nanoparticles are also produced under some ablation conditions. The TaS₂ nanoplatelets were not very stable and converted to Ta₂O₅ when exposed to air and moisture for even short periods. However, by using 3-MPA as a capping agent, the TaS₂ nanoplatelets were stabilized in aqueous solutions for over 1 week.

ACKNOWLEDGMENTS

This work was supported by the National Science Foundation (Grant No. DMR 0107429). Dr. Paul Schroeder and Jerimiah Forsythe are acknowledged for the design of the reaction chamber. Technical support from Dr. Sandeep Kohli from Colorado State University is also acknowledged.

REFERENCES

1. A.D. Yoffe and J.A. Wilson: The transition metal dichalcogenides: Discussion and interpretation of observed optical, electrical and structural properties. *Adv. Phys.* **18**, 193 (1968).
2. R. Tenne, L. Margulis, M. Genut, and G. Hodes: Polyhedral and cylindrical structures of tungsten disulfide. *Nature* **360**, 444 (1992).
3. R. Tenne, M. Homyonfer, and Y. Feldman: Nanoparticles of layered compounds with hollow cage structures (inorganic fullerene-like structures). *Chem. Mater.* **10**, 3225 (1998).
4. C.N.R. Rao and M. Nath: Inorganic nanotubes. *Dalton Trans.* **1**, 1 (2003).
5. Q. Li, E.C. Walter, W.E. van der Veer, B.J. Murray, J.T. Newberg, E.W. Bohannon, J.A. Switzer, J.C. Hemminger, and R.M. Penner: Molybdenum disulfide nanowires and nanoribbons by electrochemical/chemical synthesis. *J. Phys. Chem. B* **109**, 3169 (2005).
6. A. Carlsson, M. Brorson, and H. Topsoe: Morphology of WS₂ nanoclusters in WS₂/C hydrodesulfurization catalysts revealed by high-angle annular dark-field scanning transmission electron microscopy (HAADF-STEM) imaging. *J. Catal.* **227**, 530 (2004).
7. L.M. Kulikov, A.A. Semenov-Kobzar, K.E. Grinkevich, I.A. Kosko, L.G. Aksel'rud, and L.P. Romaka: Dispersion of transition-metal dichalcogenides and their intercalation compounds. *Inorg. Chem.* **33**, 1008 (1997).
8. M. Remskar, Z. Skraba, R. Sanjines, and F. Levy: MoS₂ and WS₂ nanotubes alloyed with gold and silver. *Surf. Rev. Lett.* **6**, 1283 (1999).
9. L. Rapoport, Y. Leshchinsky, Y. Volovik, M. Lvovsky, O. Nepomnyashchy, Y. Fieldman, R. Popovitz-Biro, and R. Tenne: Modification of contact surfaces by fullerene-like solid lubricant nanoparticles. *Surf. Coat. Technol.* **405**, 164 (2003).
10. C.M. Zelenski and P.K. Dorhout: Template synthesis of near-monodisperse microscale nanofibers and nanotubules of MoS₂. *J. Am. Chem. Soc.* **120**, 734 (1998).
11. L. Qiu, V.G. Pol, Y. Wei, and A. Gedanken: A two-step process for the synthesis of MoTe₂ nanotubes: Combining a sonochemical technique with heat treatment. *J. Mater. Chem.* **13**, 2985 (2003).
12. C. Schuffenhauer, B. Parkinson, N.Y. Jin-Phillipp, L. Joly-Portuz, J. Martin, R. Popovitz-Biro, and R. Tenne: Synthesis of fullerene-like tantalum disulfide nanoparticles by a gas-phase reaction and laser ablation. *Small* **1**(11), 1100 (2005).
13. M. Jose-Yacaman, H. Lopez, P. Santiago, D.H. Galvan, I.L. Garzon, and A. Reyes: Studies of MoS₂ structures produced by electron irradiation. *Appl. Phys. Lett.* **69**, 1065 (1996).
14. P.A. Parilla, A.C. Dillon, K.M. Jones, G. Riker, D.L. Schulz, D.S. Ginley, and M.J. Heben: The first true inorganic fullerene? *Nature* **397**, 6715 (1999).
15. R. Sen, A. Govindaraj, K. Suenaga, S. Suzuki, H. Kataura, S. Iijima, and Y. Achiba: Encapsulated and hollow closed-cage structures of WS₂ and MoS₂ prepared by laser ablation at 450–1050°C. *Chem. Phys. Lett.* **340**, 242 (2001).
16. M. Nath, C.N.R. Rao, R. Popovitz-Biro, A. Albu-Yaron, and R. Tenne: Nanoparticles produced by laser ablation of HfS₃ in liquid medium: Inorganic fullerene-like structures. *Chem. Mater.* **16**, 2238 (2004).
17. Y. Rosenfeld-Hacohen, R. Popovitz-Biro, Y. Prior, S. Gemming, G. Seifert, and R. Tenne: Synthesis of NiCl₂ nanotubes and fullerene-like structures by laser ablation: Theoretical considerations and comparison with MoS₂ nanotubes. *Phys. Chem. Chem. Phys.* **5**, 1644 (2003).
18. V. Chikan and D.F. Kelley: Size-dependent spectroscopy of MoS₂ nanoclusters. *J. Phys. Chem. B* **106**, 3794 (2002).
19. S. Yang and D.F. Kelley: The spectroscopy of InSe nanoparticles. *J. Phys. Chem. B* **109**, 12701 (2005).
20. V. Carre, F. Aubriet, P.T. Scheepers, G. Krier, and J.F. Muller: Potential of laser ablation and laser desorption mass spectrometry to characterize organic and inorganic environmental pollutants on dust particles. *Rapid Commun. Mass Spectrom.* **19**, 871 (2005).
21. C.V. Ramana, R.J. Smith, O.M. Hussain, M. Massot, and C.M. Julien: Surface analysis of pulsed laser-deposited V₂O₅ thick films and their lithium intercalated products studied by Raman spectroscopy. *Surf. Interface Anal.* **37**, 406 (2005).
22. H.W. Kroto, J.R. Heath, S.C. O'Brein, and R.E. Smalley: C₆₀: buckminsterfullerene. *Nature* **318**, 162 (1985).
23. P.A. Parilla, A.C. Dillon, B.A. Parkinson, K.M. Jones, J. Alleman, G. Riker, D.S. Ginley, and M.J. Heben: Formation of nanooctahedra in molybdenum disulfide and molybdenum diselenide using pulsed laser vaporization. *J. Phys. Chem. B* **108**, 6197 (2004).
24. Orthorhombic TaS₂, a = 5.7500 Å, b = 3.30800 Å, c = 23.76000 Å (Powder Diffraction Files-2, Vol. 47, issue 6A, June 97, card number 83-48) Hexagonal (Rh) TaS₂, a = 3.3400 Å, b = 3.3400 Å, c = 35.9400 Å (Powder Diffraction Files-2, Vol. 97, issue 6A, June 97, card number 85-48).
25. N.K. Chaki and K.P. Vijaymohan: Temperature-induced phase transitions of the ordered superlattice assembly of Au nanoclusters. *J. Phys. Chem. B* **109**, 2552 (2005).
26. Z. Peng, T. Walther, and K. Kleiner: Influence of intense pulsed laser irradiation on optical and morphological properties of gold nanoparticle aggregates produced by surface acid-base reactions. *Langmuir* **21**, 4249 (2005).